Journal of Ceramic Processing Research. Vol. 8, No. 4, pp. 256~260 (2007)

J O U R N A L O F
Ceramic Processing Research

Synthesis and luminescent properties of rare earth-doped YVO_4 nanocrystalline powders

Heesun Yang[a,*], Sooyeon Seo[b], Mostafa Abboudi[c] and Paul H. Holloway[b]

[a]*Department of Materials Science and Engineering, Hongik University, Seoul 121-791, Korea*
[b]*Department of Materials Science and Engineering, University of Florida, Gainesville, Florida 32611-6400, USA*
[c]*Universite Abdelmalek Essaadi, Faculte des Sciences, BP 2121, Tetouan 93000, Morocco*

A presentation is given of large scale rare earth-doped YVO_4 nanocrystalline powders synthesized using an organic acid-based easy, soft chemistry. First, V_2O_5 precursor was reduced (from V^{5+} to V^{4+}) in the presence of oxalic acid at 200 °C, forming oxalate compounds. Subsequent addition of yttrium nitrate and rare earth (Er or Nd) nitrate mixed with citric acid and the reaction of the resulting mixture at 400 °C led to Er- (or Nd-) doped YVO_4 nanocrystalline powders. Photoluminescent properties (emission and excitation) of near infrared (NIR) ($^4I_{11/2} \rightarrow {}^4I_{15/2}$) emitting nanocrystalline YVO_4:Er phosphor were characterized as a function of the Er concentration and post-annealing temperature. Characteristic NIR ($^4F_{3/2} \rightarrow {}^4I_{11/2}$) emission of nanocrystalline YVO_4:Nd phosphor is also reported.

Key words: rare earth, YVO_4 nanocrystalline, near infrared, concentration, post-annealing.

Introduction

Luminescent oxide materials, which are found in a number of devices including display phosphors, lamps, and lasers, have been investigated at the nanometre dimension [1, 2]. Numerous luminescent nanoparticles ranging from visible light to infrared can be achieved by introducing transition metal or rare earth elements into II-VI semiconductors or oxides. Near infrared (NIR) emitting nanocrystalline oxides can be promising in potential applications such as biological labels and integrated optical circuitry (for light amplifiers and for optical fiber communication) [3-5].

NIR emissions at wavelengths of 1.3 and 1.5 μm are, in particular, useful in standard silica-based telecommunication fibers due to their low transmission loss [5]. Trivalent erbium (Er) and neodymium (Nd) ions are well known to be NIR luminescent centers for 1.3 and 1.5 μm, respectively [4-6]. In these rare earth ions, electrons in the partially filled 4*f* inner shell are shielded by outer shells of completely filled $5s^2$ and $5p^6$. Emissions are due to a 4*f*-4*f* intraband transition for the Er^{3+} ion and both 4*f*-4*f* intraband and 5*d*-4*f* interband transitions for the Nd^{3+} ion [7]. Due to the good shielding of the incompletely filled 4*f* electrons from the chemical environment, the *f-f* transition is not influenced by external crystal fields, leading to a sharp, distinct characteristic emission line of the *f-f* transition. Energy levels and corresponding emission lines for Er^{3+} and Nd^{3+} ions are shown in Fig. 1.

Yttrium orthovanadate (YVO_4) has been a promising host material for a variety of optical applications including as a phosphor, a laser host, and infrared polarizer due to its mechanical and optical properties [9, 10]. The high quantum efficiency (70%) of bulk Eu^{3+}-doped YVO_4 motivated the investigation of its nanocrystalline form [11, 12]. In addition, other trivalent rare earth-doped oxide nanocrystalline systems such as lanthanide phosphate ($LaPO_4$:Er^{3+}, Nd^{3+}, or Pr^{3+}) were successfully synthesized using a wet colloid chemistry [2, 4] and showed reasonable NIR emissions.

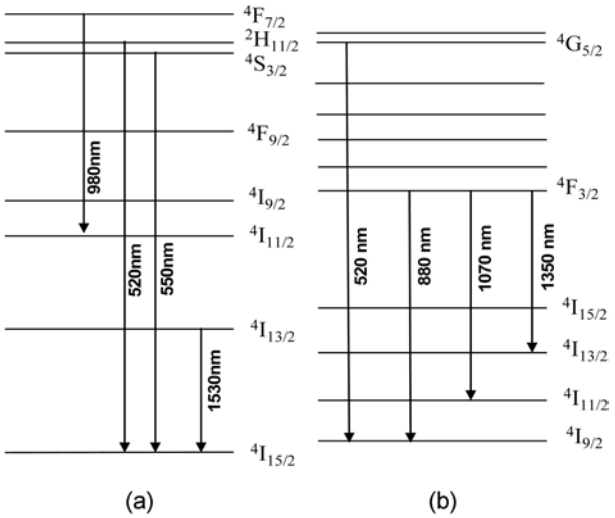

Fig. 1. Schematics of energy levels of (a) Er^{3+} and (b) Nd^{3+} ions [7, 8].

*Corresponding author:
Tel : +82-320-3039
Fax: +82-333-0127
E-mail: hyang@hongik.ac.kr

In this study, large scale synthesis of Er^{3+}-or Nd^{3+}-doped YVO_4 nanocrystalline powders is demonstrated using an easy, soft chemistry, in which organic acids are used [13]. We focus on the structural and luminescent (visible and infrared) properties of YVO_4:Er nanocrystalline samples. The effects of Er^{3+} concentration and annealing temperature on the luminescent properties of YVO_4:Er nanocrystalline powders are reported, and Nd^{3+}-doped YVO_4 nanocrystalline samples are also demonstrated.

Experimental Procedure

For the production of Er^{3+}-or Nd^{3+}-doped YVO_4 nanocrystalline powders, the synthesis basically consists of two steps [13]; first, the V_2O_5 precursor was reduced (from V^{5+} to V^{4+}), forming oxalate compounds, in the presence of oxalic acid ($H_2C_2O_4$) and water at 200 °C as shown in the following reactions:

$$H_2C_2O_4 + 2H_2O \rightarrow 2H_3O^+ + 2CO_2 + 2e^- \quad (1)$$

$$V_2O_5 + 2e^- + 6H_3O^+ \rightarrow 2VO^{2+} \text{ (or } V^{4+}) + 9H_2O \quad (2)$$

Electrons generated by the oxalic acid are used for the reduction of V_2O_5. During the V_2O_5 reduction process, the color of the powder mixture changed from dark brown to dark blue due to the transition from V^{5+} to V^{4+}. In the second step, yttrium nitrate and rare earth (Er or Nd) nitrate mixed with citric acid ($C_6H_8O_7$) and water were added into the above oxalate compounds, and the resulting mixture was reacted at 200 °C. In this step, yttrium nitrate and rare earth nitrate form complexes with the citric acid as in the following reaction:

$$2M(NO_3)_3 + 12C_6H_8O_7 \rightarrow M_2(C_6H_8O_7)_3 + 18CO_2 + 6NO + 8H_2O, \text{ where M=Y, Er, Nd} \quad (3)$$

In a typical synthesis of YVO_4:Er nanocrystalline powder, 0.005 mol of V_2O_5 (99.5%) was mixed with 0.02 mol of oxalic acid and 5 ml of deionized water in a mortar, and this mixture was raised to 200 °C for 30 minutes. 1, 2, 5 and 10 mol % of $Er(NO_3)_3{\cdot}5H_2O$ (99.99 %) in 0.0099 mol of $Y(NO_3)_3{\cdot}6H_2O$ (99.999%) were mixed and ground with 0.02 mol of citric acid and the above oxalate compound to achieve homogeneity. The resulting mixture was reacted at 200 °C for 1 h and further raised to 400 °C for another 1 h. The same procedure for the preparation of Nd-doped YVO_4 nanocrystalline powders was employed using $Nd(NO_3)_3{\cdot}6H_2O$ (99.99%). The as-synthesized nanocrystalline powders were post-annealed at 700-900 °C for 2 h in an air atmosphere.

Visible and near infrared (NIR) photoluminescence (PL) emission and excitation (PLE) spectra of YVO_4:Er and YVO_4:Nd nanocrystalline samples were collected at room temperature using a silicon-based photomultiplier tube (PMT) and a thermoelectrically cooled germanium (Ge) photodiode, respectively, and using a monochromatized 300 W Xe light source (PL set-up I). A different PL set-up (PL set-up II), consisting of a HeCd laser (325 nm) excitation source and PMT/Ge photodiode, was also used to collect highly-resolved emission spectra. Powder X-ray diffraction (XRD) spectra were collected in the step mode, by a Philips APD 3720 X-ray powder diffractometer with Cu K_α radiation. A JEOL 2010F transmission electron microscope operated at 200 kV was used for collection of images of nanocrystalline samples.

Results and Discussion

PL measurements on 1 mole % Er-doped YVO_4 nanocrystalline powders, annealed at 900 °C for 2 h, were carried out. First, visible (green) emissions (Fig. 2(a)) at 520 and 550 nm were observed due to the Er transitions of $^2H_{11/2} \rightarrow {}^4H_{15/2}$ and $^4S_{3/2} \rightarrow {}^4H_{15/2}$, respectively, as illustrated in Fig. 1(a). A PL excitation (PLE) spectrum (Fig. 2(b)) was collected with the detected wavelength of 550 nm, showing that the excitation band peaks at 320 nm. Secondly, an NIR emission spectrum of the same sample was collected with the excitation of 320 nm, exhibiting a characteristic NIR emission at 1530 nm due to $^4I_{13/2} \rightarrow {}^4I_{15/2}$ transition, as shown in Fig. 3(a). In addition, a shorter wavelength region (980-1000 nm) from $^4F_{7/2} \rightarrow {}^4I_{11/2}$ transition was also observed with a weak intensity. The excitation spectrum (Fig. 3(b)) for NIR emission consists of an excitation band with a peak at 320 nm and other lines (510, 650, and 770 nm caused by direct excitation of Er^{3+} *f-f* transitions) with the detected wavelength of 1530 nm. The PL and PLE spectra in Figs. 2 and 3 were recorded with the PL set-up I. The excitation band with a peak at 320 nm for both visible and NIR emissions is attributed to the

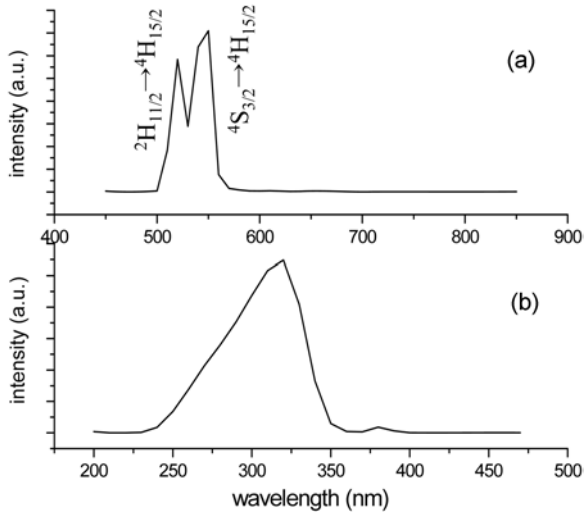

Fig. 2. Visible (a) PL emission and (b) excitation spectra of YVO_4:Er (1 mole %) nanocrystalline powders post-annealed at 900 °C for 2 h. The excitation wavelength in (a) and detected wavelength in (b) are 320 and 550 nm, respectively.

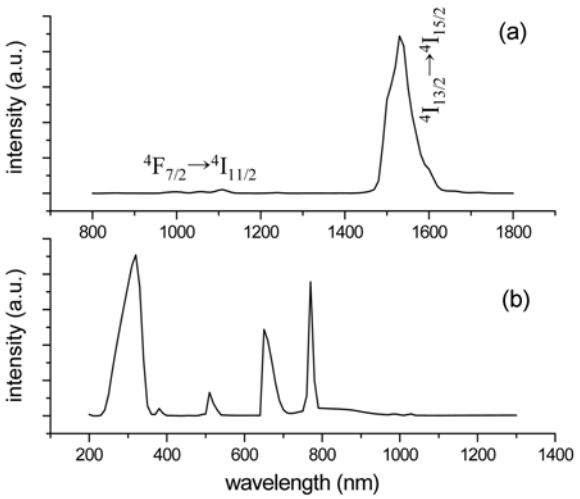

Fig. 3. NIR (a) PL emission and (b) excitation spectra of YVO_4:Er (1 mole %) nanocrystalline powders post-annealed at 900 °C for 2 h. The excitation wavelength in (a) and detected wavelength in (b) are 320 and 1540 nm, respectively.

YVO_4 host absorption. It has been speculated that the excitation is due to the filled oxygen 2*p* levels in the valence band being excited to the empty vanadium 3*d* levels of the conduction band [14]. The excitation process can be explained as in Eu^{3+}-doped YVO_4 bulk or nanocrystalline samples in the literature [12, 14, 15]. Ultra violet excitation light is absorbed by the VO_4^{3-} groups present in the YVO_4 host and the excitation energy is transferred to nearby Er ions in a non-radiative fashion. Subsequently, an Er ion in the excited state relaxes back to the ground state through a radiative transition.

The effects of the post-annealing temperature on the photon emission were investigated with 1 mole % Er-doped YVO_4 samples. As-synthesized, 700, and 800 °C annealed samples barely emitted NIR (Fig. 4(a)) as well as visible light (not shown here) due to the poor crystallinity. The 900 °C-annealed sample, however, exhibited a significant intensity of NIR emission as shown in Fig. 4(a). Unlike the NIR emission spectrum in Fig. 3(a), the finer structure of the Er^{3+} luminescence could be obtained by using the PL set-up II including a 325 nm HeCd laser excitation source. The fine structure of the $^4I_{13/2}\rightarrow{}^4I_{15/2}$ transition is caused by the thermal population of the different split $^4I_{13/2}$ levels [8]. It seems that there was practically no thermal quenching up to room temperature. A powder XRD pattern of YVO_4:Er (1 mole %) annealed at 900 °C for 2 h is shown in Fig. 4(b). The XRD pattern of the nanocrystalline powders is consistent with the tetragonal zircon structure from bulk YVO_4 (17-0341 Joint Committee on Powder Diffraction Standards file) [14, 15], excluding the possibility of the formation of secondary phases such as $Y_8V_2O_{17}$. The mean size of nanoparticles ~45 nm in diameter was calculated from the Debye-Scherrer formula. The TEM image in the inset of Fig. 4(b) shows YVO_4:Er

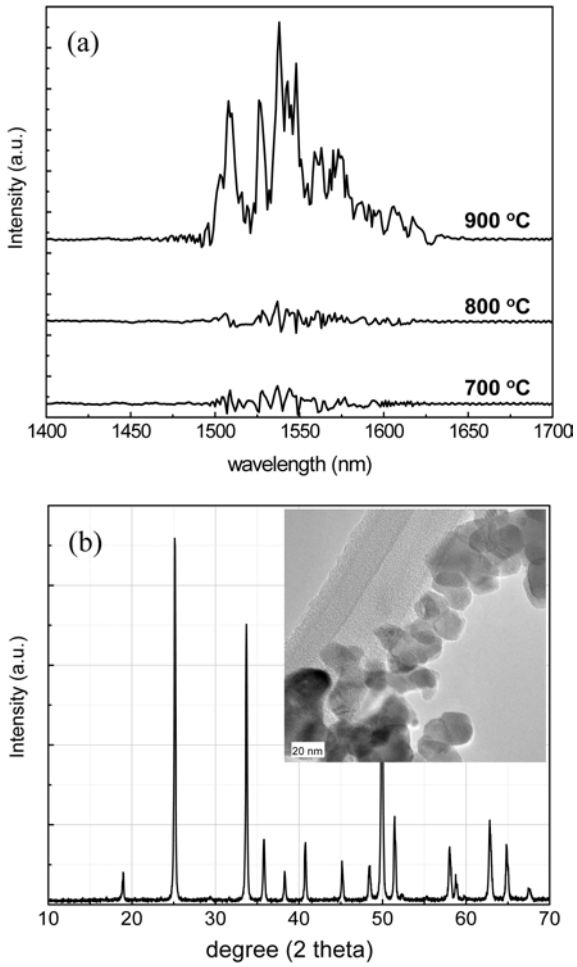

Fig. 4. (a) NIR emissions of characteristic Er^{3+} $^4I_{13/2}\rightarrow{}^4I_{15/2}$ transition as a function of post-annealing temperature. 325 nm HeCd laser was used as an excitation source with PL set-up II. (b) Powder XRD pattern of YVO_4:Er nanocrystalline powders annealed at 900 °C for 2 h. The inset in (b) represents TEM image of the same sample and the scale bar in the image is 20 nm.

nanoparticles (annealed at 900 °C for 2 h) distributed from 20 nm to larger sizes in diameter.

Visible ($^2H_{11/2}\rightarrow{}^4H_{15/2}$ and $^4S_{3/2}\rightarrow{}^4H_{15/2}$) and NIR ($^4I_{13/2}\rightarrow{}^4I_{15/2}$) emissions of YVO_4:Er nanocrystalline phosphors with different Er concentrations from 1 to 10 mole % were collected using a 325 nm HeCd laser excitation source, as shown in Fig. 5. In general, intensities of both emissions show a similar trend as a function of Er concentration, indicating maximum intensities at 1 mole % of Er activator and thus the occurrence of concentration quenching at higher Er concentrations above 1 mole %. Note that sharper and finer spectra for both visible and NIR emission were obtained using PL set-up II versus PL set-up I used for Figs. 2 and 3. It has been reported that in bulk or nanocrystalline YVO_4:Eu phosphors a maximum luminescence intensity is found at ~5 mole % of Eu activator, above which concentration quenching occurs due to the high probability of energy transfer between Eu ions [15]. This partial quenching of the luminescence by a

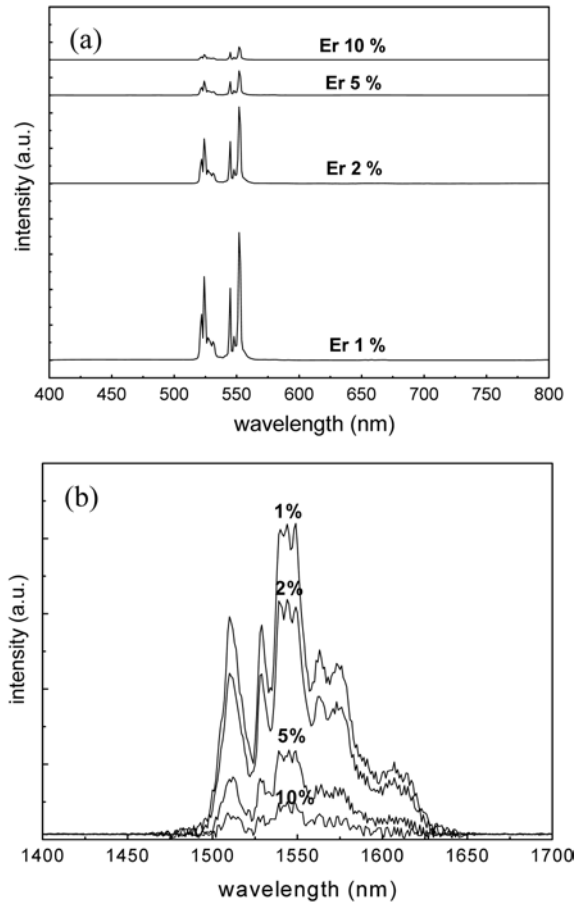

Fig. 5. Variation of (a) visible and (b) NIR emissions of YVO_4:Er nanocrystalline samples as a function of Er concentration. The spectra were recorded with PL set-up II.

high concentration of activator is a typical phenomenon in the lanthanide-doped phosphor systems, depending on the types of lanthanide and host systems.

In addition to YVO_4:Er nanocrystalline powders, 0.5 mole % Nd-doped YVO_4 nanocrystalline powders were prepared using Nd (III) nitrate with the same synthetic chemistry and post-annealing procedure (900 °C for 2 h). Visible and NIR emissions (excited by 320 nm) collected with the PL set-up I are shown in Fig. 6(a) and (b), respectively. The green emission (520 nm) is due to the Nd^{3+} $^4G_{5/2} \rightarrow {}^4H_{9/2}$ transition and NIR emissions at 880, 1070, and 1350 nm are characteristic Nd^{3+} transition lines due to $^4F_{3/2} \rightarrow {}^4I_{9/2}$, $^4F_{3/2} \rightarrow {}^4I_{11/2}$, and $^4F_{3/2} \rightarrow {}^4I_{13/2}$, respectively, as illustrated in Fig. 1(b). The finer structure of the Nd^{3+} NIR emission, obtained from the PL set-up II, is also shown in Fig. 6(c). PLE spectra of visible and NIR emission were collected with the PL set-up I, and a very similar excitation band peaking at 320 nm was observed with that of YVO_4:Er nanocrystalline sample. Powder XRD patterns and TEM images (not shown here) were collected from the YVO_4:Nd sample, but were in general the same as those from the YVO_4:Er sample, indicating that the activators used do not affect the crystal structure and morphology.

Conclusions

Rare earth-doped YVO_4 nanocrystalline powders were successfully prepared using a new low temperature-based chemistry, in which organic polyacids such as oxalic acid and citric acid are used. Visible and NIR emissions of nanocrystalline YVO_4:Er phosphors were characterized as a function of the Er concentration (1-10 mole %) and post-annealing temperature (700-900 °C). Characteristic visible and NIR emissions of nanocrystalline YVO_4:Nd phosphors were also demonstrated. Beyond Er- or Nd-doped YVO_4 nanocrystalline powders reported here, a variety of rare earth-doped oxide phosphors or even other types of oxides (i.e., non-phosphors) can be prepared into a nanocrystalline form with the synthetic chemistry used in this study. A red emitting Eu^{3+}-doped $ZnGa_2O_4$ phosphor, an ionic conducting $Ce_{1-x}La_xO_{2-x/2}$, and iron oxides (α-Fe_2O_3, γ-

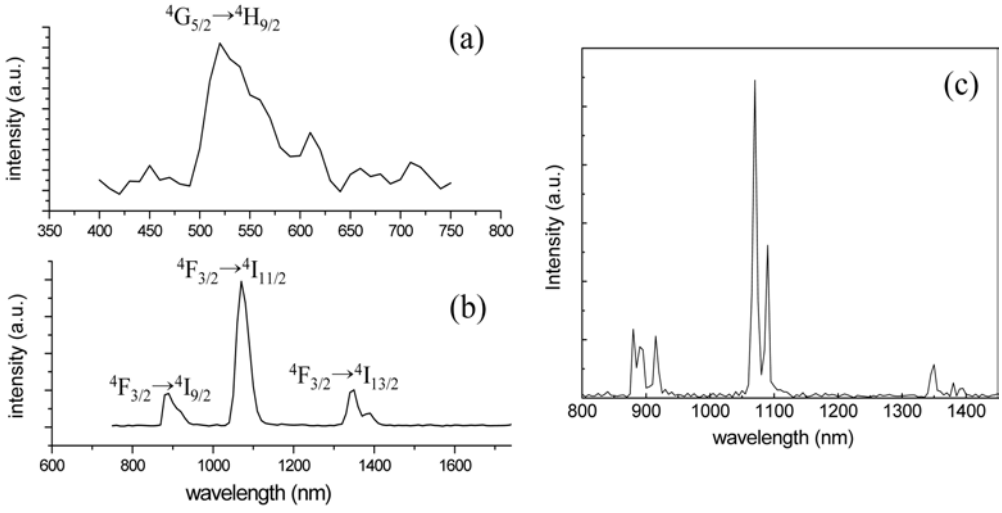

Fig. 6. (a) visible and (b) NIR emission spectra of YVO_4:Nd nanocrystalline powders collected with PL set-up I. Both emissions were recorded with an excitation wavelength of 320 nm. (c) NIR emission spectrum collected with PL set-up II.

Fe_2O_3) in a nanocrystalline form are good examples which are currently under investigation [13].

Acknowledgment

This work was supported by Seoul Research and Business Development Program (10555) and ARO Grant DAAD19-01-1-0603 and ARL Grant W911NF-04-200023. This work was also supported by 2006 Hongik University Research Fund.

References

1. H. Guo, N. Dong, M. Yin, W. Zhang, L. Lou, and S. Xia, J. Phys. Chem. B 108 (2004) 19205-19209.
2. O. Lehmann, H. Meyssamy, K. Kompe, H. Schnablegger, and M. Haase, J. Phys. Chem. B 107 (2003) 7449-7453.
3. V. Buissette, A. Huignard, T. Gacoin, J. Boilot, P. Aschehoug, and B. Viana, Surf. Sci. 532 (2003) 444-449.
4. G. Hebbink, J. Stouwdam, D. Reinhoudt, and F. van Veggel, Adv. Mater. 14 (2002) 1147-1150.
5. J. Kim and P. Holloway, Adv. Mater. 17 (2005) 91-96.
6. A. Georgobiani, A. Gruzintsev, T. Nikiforova, C. Barthou, and P. Benalloul, Inorg. Mater. 38 (2002) 1008-1011.
7. A. Kale, N. Shepherd, W. Glass, D. DeVito, M. Davidson, and P. Holloway, J. Appl. Phys. 94 (2003) 3147-3152.
8. A. Georgobiani, A. Gruzintsev, C. Barthou, P. Benalloul, J. Benoit, B. Tagiev, O. Tagiev, and R. Dzhabborov, J. Electrochem. Soc. 148 (2001) H167-170.
9. G. Blasse and A. Bril, J. Chem. Phys. 48 (1968) 217-222.
10. G.E. Venikousa and R.C. Powell, Phys. Rev. B 17 (1978) 3456-3461.
11. A. Huignard, V. Buissette, G. Laurent, T. Gacoin, and J. Boilot, Chem. Mater. 14 (2002) 2264-2269.
12. A. Huignard, T. Gacoin, and J. Boilot, Chem. Mater. 12 (2000) 1090-1094.
13. M. Abboudi and P.H. Holloway, U.S. Patent, November 2006, 7,135,161 B2.
14. J. Kang, M. Nazarov, W. Bin Im, J. Kim, and D. Jeon, J. Vac. Sci. Technol. B 23 (2005) 843-848.
15. K. Riwotzki and M. Haase, J. Phys. Chem. B 102 (1998) 10129-10135.